Int. J. Solids Structures Vol. 18, No. 10, pp. 873–881, 1982
Printed in Great Britain.

0020-7683/82/100873-09$03.00/0
Pergamon Press Ltd.

THE INITIATION OF CREEP CRACK GROWTH

R. A. AINSWORTH
Central Electricity Generating Board, Berkeley Nuclear Laboratories, Berkeley, Gloucestershire GL13 9PB, England

(*Received* 23 *November* 1981)

Abstract—The blunting of a crack tip under creep conditions is investigated using an approximate analysis which assumes that the crack blunts into a semi-circular shape. The rate of crack opening displacement is determined as a function of applied load and the material creep strain rate law. The time to initiate growth of the crack is expressed in terms of the crack opening displacement at initiation and the result is compared with experimental data.

1. INTRODUCTION

The creep failure time of defect-free structures may be predicted by entering the stress/time-to-rupture curve of the material at a reference stress based on limit analysis[1]. This result holds provided the material is creep ductile[2] and is remarkably simple when one considers that the mechanism of structural failure is complex, involving the initiation and spreading of zones of creep-damaged material (material in the tertiary stage of creep) through the structure[3]. In cracked components, provided crack growth is slower than the growth of the damage zone ahead of the crack, the simple result still holds and the failure time may be obtained from the reference stress based on the initial crack length[4].

When the crack growth rate exceeds the propagation rate of the damage zone it is necessary to allow for crack extension when calculating the failure time. Experimental values of crack growth rate have been correlated with elastic stress intensity factor, reference stress and the contour integral C^* by a number of authors. The data has been reviewed by Haigh[5] and by Ellison and Harper[6]. Ainsworth[7] has indicated the ranges of crack velocity for which various correlations are appropriate and for which failure time is governed by the reference stress. In addition to an expression for crack growth rate it is necessary to know the time at which crack growth starts in order to predict the failure time. Although an underestimate of failure time may be obtained by assuming that crack growth starts immediately after loading, this can be unduly pessimistic as the initiation or incubation time can occupy a significant fraction of the total life (e.g. [8]).

The present paper considers initiation of crack growth by examining the progressive blunting of a crack tip in creep. Since experimental evidence (e.g. [8]) suggests that crack initiation may be described by the attainment of a critical crack opening displacement (COD) the analysis is used to relate the initiation time to the COD at initiation. The result is compared with experimental data.

2. BLUNTING OF A CRACK TIP IN CREEP

2.1 *Material behaviour*

In calculating the progressive blunting of the crack a simple secondary creep law is used and elastic and plastic strains are neglected. Thus at each instant the stress and strain-rate fields are the steady-state fields for the current deformed geometry of the crack tip. The effects of including elastic, plastic and primary creep strains are discussed in sub-section 2.3. The secondary creep law is

$$\dot{\epsilon}_{ij} = \frac{3}{2}\dot{\epsilon}_0(\sigma_e/\sigma_0)^{n-1}S_{ij}/\sigma_0 \tag{1}$$

where $\dot{\epsilon}_{ij}$ is the creep strain rate tensor, σ_e and S_{ij} are related to the stress tensor σ_{ij} by

$$S_{ij} = \sigma_{ij} - \frac{1}{3}\delta_{ij}\sigma_{kk}, \quad \sigma_e^2 = \frac{3}{2}S_{ij}S_{ij}$$

and n, σ_0, $\dot{\epsilon}_0$ are constants. The creep energy dissipation rate is

$$\dot{W} = \int \sigma_{ij}\, \mathrm{d}\dot{\epsilon}_{ij} = \frac{n}{(n+1)}\sigma_{ij}\dot{\epsilon}_{ij} = \frac{n}{(n+1)}\sigma_0\dot{\epsilon}_0(\sigma_e/\sigma_0)^{n+1}. \tag{2}$$

2.2 *Crack blunting*

It is assumed that the crack tip blunts into a semi-circular shape as shown in Fig. 1. Plane strain conditions are assumed. Following Rice ([9], p. 242) the strain rates on the notch surface may be estimated by assuming that they are compatible with a homogeneous strain rate $\dot{\epsilon}_{yy}$ within the notch. Then

$$\dot{\epsilon}_{\theta\theta} \simeq \dot{\epsilon}_{yy} \cos^2 \theta. \tag{3}$$

The effect on the result of assuming that the hoop strain rate is constant on the notch surface ($\dot{\epsilon}_{\theta\theta} = \dot{\epsilon}_{yy}$) is discussed later. The amplitude $\dot{\epsilon}_{yy}$ of the strain rate may be determined in terms of the creep integral C^* in the same manner as Rice ([9], p. 290) determined the elastic–plastic solution in terms of J. The C^* integral is defined by

$$C^* = \int_\Gamma \{\dot{W}\, \mathrm{d}y - \sigma_{ij}\partial\dot{u}_j/\partial x\, \mathrm{d}s_j\}$$

where (x, y) are co-ordinates defined with respect to the crack as in Fig. 1, $\dot{u}_i$ are displacement rates and $\mathrm{d}s_i$ is an element of Γ which is a path, traversed anticlockwise, which encloses the crack tip. The integral is independent of the choice of the path Γ. Taking a path along the crack surface from B to A in Fig. 1 noting that the tractions are zero on the surface gives

$$C^* = \int_{-\pi/2}^{\pi/2} \dot{W}\, a \cos\theta\, \mathrm{d}\theta$$

Substituting for $\dot{W}$ from eqns (1)–(3) noting plane strain conditions this becomes

$$C^* = \frac{n}{n+1}\sigma_0\dot{\epsilon}_0 a \int_{-\pi/2}^{\pi/2} \left(\frac{2\dot{\epsilon}_{yy}\cos^2\theta}{\sqrt{(3)}\dot{\epsilon}_0}\right)^{1+1/n} \cos\theta\, \mathrm{d}\theta$$

$$= \frac{n}{n+1}\sigma_0\dot{\epsilon}_0 a (2\dot{\epsilon}_{yy}/\sqrt{(3)}\dot{\epsilon}_0)^{1+(1/n)} \Gamma\left(\frac{1}{2}\right)\Gamma\left(2+\frac{1}{n}\right)/\Gamma\left(2\frac{1}{2}+\frac{1}{n}\right)$$

whence

$$\dot{\epsilon}_{yy} a^{n/n+1} = \frac{\sqrt{3}}{2}\dot{\epsilon}_0 \left[\frac{C^*}{\sigma_0\dot{\epsilon}_0} \frac{\Gamma(5/2+1/n)}{\Gamma\left(\frac{1}{2}\right)\Gamma(1+1/n)}\right]^{n/n+1}. \tag{4}$$

This corresponds to the solution of Rice ([9], p. 292) for a power law plastic hardening material. The ratio of gamma functions may be very accurately represented at large n by

$$\Gamma\left(\frac{5}{2}+\frac{1}{n}\right)/\Gamma\left(\frac{1}{2}\right)\Gamma\left(1+\frac{1}{n}\right) \simeq \frac{3}{4}+\frac{1}{n}. \tag{5}$$

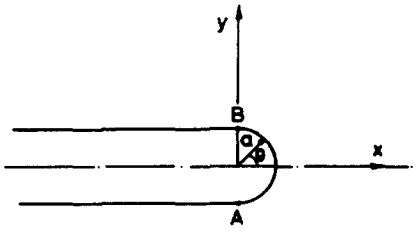

Fig. 1. Geometry of blunted crack tip.

(The asymptotic expansion as $n \to \infty$ is $0.75 + 0.96/n + 0(1/n^2)$; eqn (5) is a good approximation even for small n with an error, for example, of less than 2% at $n = 2$, and enables a simple formula to be developed for the initiation time). The strain rate $\dot{\epsilon}_{yy}$ may be approximately related to the rate of crack opening between A and B in Fig. 1 as $\dot{\epsilon}_{yy} = \dot{a}/a$ so that eqn (4) becomes, on noting (5),

$$a^{-1/(n+1)}\dot{a} = \frac{\sqrt{3}}{2}\dot{\epsilon}_0\left[\frac{C^*}{\sigma_0\dot{\epsilon}_0}\frac{(3n+4)}{4n}\right]^{n/n+1}. \tag{6}$$

It has been assumed here that the notch retains its semi-circular shape with radius equal to one-half of the opening displacement between A and B although the strain-rate field of eqn (3) would not lead to such a uniform increase in radius. If, alternatively, a uniform hoop strain rate had been assumed as being more consistent with the retention of a semi-circle, the factor of $(3n+4)/4n$ in eqn (6) would be replaced by $(n+1)/2n$. The choice between these two approximations is somewhat arbitrary but eqn (6) is retained here on the basis that eqn (3) is probably a better representation of the strain-rate distribution.

For constant loading C^* can be taken as approximately constant provided the COD is small compared with the crack length and other component or specimen dimensions (e.g. remaining ligament). Equation (6) can then be integrated to give the initiation time t_i in terms of the COD at initiation ($\delta_i = 2a_i$) and the notch opening, δ_0, at time $t = 0$,

$$\delta_i^{n/n+1} - \delta_0^{n/n+1} = \frac{\sqrt{(3)}n\dot{\epsilon}_0 t_i}{2(n+1)}\left[\frac{C^*}{\sigma_0\dot{\epsilon}_0}\frac{3n+4}{2n}\right]^{n/n+1}. \tag{7}$$

When the notch opening after initial loading is small ($\delta_0 \ll \delta_i$) the initiation time is related to δ_i by

$$t_i = \frac{2(n+1)}{n\sqrt{(3)}\dot{\epsilon}_0}\left[\frac{2n\sigma_0\dot{\epsilon}_0\delta_i}{(3n+4)C^*}\right]^{n/n+1}. \tag{8}$$

When δ_0 is not negligible, for example for an initially spark-machined slot, δ_i in eqn (8) can simply be replaced by an effective initiation COD $\bar{\delta}_i$

$$\bar{\delta}_i = (\delta_i^{n/n+1} - \delta_0^{n/n+1})^{1+1/n}. \tag{9}$$

The result of eqn (8) may be expressed in a more convenient form by introducing the reference stress

$$\sigma_{ref} = \frac{P}{P_0(\sigma_0)}\sigma_0 \tag{10}$$

where P is the applied load and $P_0(\sigma_0)$ is the collapse load calculated for a perfectly plastic material of yield stress σ_0. With this definition the creep integral C^* may be related to the applied loading by

$$C^* = \sigma_{ref}\dot{\epsilon}(\sigma_{ref})R \tag{11}$$

where R is a characteristic macroscopic distance which may be obtained from tables (e.g. [10]) for some geometries or may be approximated in plane strain by $R = 0.75K^2/\sigma_{ref}^2$ in other cases[7]. Introducing the creep rupture time $t_r(\sigma)$ in terms of the Monkman–Grant constant $\bar{\epsilon}$ as

$$\dot{\epsilon}(\sigma)t_r(\sigma) = \bar{\epsilon} \tag{12}$$

eqn (8) becomes, after some algebraic manipulation

$$\frac{t_i}{t_r(\sigma_{ref})} = \frac{2(n+1)}{n\sqrt{(3)}\bar{\epsilon}}\left[\frac{2n}{3n+4}\frac{\delta_i}{R}\right]^{n/n+1}. \tag{13}$$

Equation (13) is the basic result of the present paper. The time $t_r(\sigma_{ref})$ is the lifetime of a structure when crack-tip events are unimportant and failure is governed by overall creep rupture mechanisms. Equation (13) then determines whether it is necessary to consider initiation and subsequent crack growth in estimating the lifetime or whether it is sufficient to simply take the lifetime as $t_r(\sigma_{ref})$. It can be seen that initiation is influenced by the conventional material properties $\bar{\epsilon}$ and n, by the initiation COD δ_i also taken as a material property, and by the geometrical factor R. Equation (13) is discussed in detail in Section 3 and its application to experimental data is given in Section 4.

2.3 *The inclusion of plastic and primary creep strains*

Equation (13) may be expressed in the form

$$\epsilon(\sigma_{ref}, t_i) = \frac{2(n+1)}{n\sqrt{3}}\left[\frac{2n}{3n+4}\frac{\delta_i}{R}\right]^{n/n+1} \tag{14}$$

where $\epsilon(\sigma_{ref}, t_i)$ is the creep strain accumulated in time t_i at the reference stress. If the effects of primary creep are represented by the inclusion of a time-hardening function in eqn (1), the time-function may be removed by a redefinition of time-scale [11] leading to the initiation time again being defined by eqn (14). This assumes the same stress dependence of both primary and secondary creep strain rate although an effective value of n appropriate to the initiation time could be adopted as suggested by Ewing[12]. The distance R defined by eqn (11) is, however, not particularly sensitive to n so that it can be seen from eqn (14) that the present result is not strongly dependent on the choice of n.

The inclusion of elastic and plastic strains in eqn (1) has two effects. First, these strains lead to a crack tip opening on initial loading and, secondly, they lead to a period of stress redistribution prior to the attainment of the steady-state creep solution. The COD on initial loading has been evaluated by McMeeking[13] using finite-elements who expressed his results as

$$\delta = (\beta J/\sigma_0)\left\{\frac{2(1+\nu)}{\sqrt{3}}(n'+1)\frac{\sigma_0}{E}\right\}^{1/n'} \tag{15}$$

where E is Young's modulus, ν is Poisson's ratio, σ_0 is the yield stress, n' is the hardening exponent in a plasticity law similar to eqn (1) and J is the value of the contour integral for the applied loading. The value of β depends on σ_0/E and n' and on the definition of how δ is measured but the finite-element results typically gave $\beta = 0.6$. When the initial loading leads to fully plastic behaviour, J is given in a similar manner to eqn (1̇1) and setting $\nu = 1/2$, eqn (15) may be expressed

$$\epsilon'(\sigma_{ref}) = \frac{1}{\sqrt{(3)}(n'+1)}\left[\frac{\sqrt{(3)}(n'+1)\delta}{\beta R}\right]^{n'/n'+1} \tag{16}$$

$$= \frac{2(n'+1)}{n'\sqrt{3}}\left[\frac{2n'}{3n'+4}\frac{\delta}{R}\right]^{n'/n'+1}\gamma(n', \beta) \tag{17}$$

where $\epsilon'(\sigma_{ref})$ is the plastic strain at the reference stress and γ is defined by eqns (16) and (17). For $\beta = 0.6$, γ varies between 0.56 and 2.17 for $1 \leq n' \leq \infty$ and between 0.86 and 1.55 for $2 \leq n' \leq 10$. As noted in[13] there are differences between the finite-element values of β and experimental values which vary from 0.44 to 1.0 for the tests quoted by McMeeking. Thus eqn (14) gives a reasonable approximation to the COD at $t = 0$ if ϵ is interpreted as the plastic strain at the reference stress. This agreement between the creep and fully plastic results must be regarded as somewhat fortuitous as the stress histories at the notch surface are completely different in the two cases: for creep the load is constant and the stress falls as the notch radius increases; for plasticity there is also an increase in notch radius but this occurs as a result of increased load and the net effect is an approximately constant stress at the notch surface. However, the fortuitous agreement does suggest that for practical purposes initial loading effects

may be included by using eqn (14) with ϵ interpreted as the total strain at the reference stress. As for primary creep strains the insensitivity of eqn (14) to n means that an effective n (evaluated, say, from the isochronous stress–strain curve at time t_i) can be used.

Fully plastic behaviour has been assumed on initial loading in expressing eqn (15) in the form of eqn (16) or (17). However, when the loading is small so that only small-scale yielding occurs, then $J = (1-\nu^2)K^2/E$ and $\epsilon(\sigma_{ref}) = \sigma_{ref}/E$. Substituting these into eqn (15) again leads to eqn (17) but with $\gamma(n, \beta)$ replaced by γ_1 where

$$\gamma_1 = \gamma(n', \beta)\left[\frac{3}{2(1+\nu)}\right]^{1/n'+1}\left[\frac{\sigma_{ref}^2 R}{K^2(1-\nu^2)}\right]^{n'/n'+1}\left(\frac{\sigma_{ref}}{\sigma_0}\right)^{-(n'-1)/(n'+1)} \tag{18}$$

As noted by Ainsworth[7], for $n = 1$, $R = 3/4K^2/\sigma_{ref}^2$ in plane strain and is not particularly sensitive to n. Thus use of eqn (14) instead of eqn (15) to predict the COD on initial loading will only lead to errors for small scale yielding when n is large and $\sigma_{ref} \ll \sigma_0$, i.e. when the load is small compared to the collapse load. From eqn (17), in these cases the value of δ/R on initial loading is very small (of order σ_{ref}/E) and will only have a significant effect when the predicted value of $t_i/t_r(\sigma_{ref})$ from eqn (13) is very small. For practical purposes initiation may be assumed to occur at $t = 0$ when the predicted value of $t_i/t_r(\sigma_{ref}) \ll 1$ and this is discussed further in Section 3 below.

The effect of neglecting stress redistribution to the steady-state creep solution may be assessed from the work of Bassani and McClintock[14] who examined redistribution from an initially elastic response. They found that the COD during the redistribution period was of order the elastic COD and that the redistribution time (t_{red}, say) was typically of order

$$t_{red} = (\sigma_{ref}/E)/\dot{\epsilon}(\sigma_{ref})$$

(see also Penny and Marriott[11] for a general discussion of redistribution times). Thus from eqn (13)

$$t_{red}/t_i \sim (\sigma_{ref}/E)/(\delta_i/R).$$

Since the elastic strain is typically less than 0.1% the redistribution time is a small fraction of t_i except when δ/R is small. Thus, as above for the COD on initial loading, redistribution effects should be small except when the predicted value $t_i/t_r(\sigma_{ref}) \ll 1$ in which case initiation may be assumed to occur at $t = 0$ for practical purposes.

3. DISCUSSION OF THE THEORETICAL RESULT

When the reference stress is defined by eqn (10) with the multi-axial yield surface chosen similar to the multi-axial creep rupture surface, the time $t_r(\sigma_{ref})$ is an upper bound on the failure time of a structure[1]. In recent years this and other developments of reference stress methods have enabled the creep design of defect-free components to be based on limit analysis[15] so providing an obvious similarity between low and high temperature design methods. For initially cracked components, Goodall and Chubb[4] have shown that when crack propagation effects are negligible the creep life of a component is still determined by the reference stress provided allowance is made for the presence of the crack in calculating the limit load. Again there is a similar result at low temperature where, at one extreme of behaviour in post-yield fracture mechanics, the reduction in load-bearing capacity of a component is determined by the reduction in the limit load due to the presence of the crack[16]. However, just as this represents only one extreme of behaviour and the load-bearing capacity may be further reduced if failure is governed by crack tip events[16], so the load-bearing capacity at elevated temperature may be further reduced if failure is governed by the initiation and growth of a dominant creep crack.

The analysis of the previous section as expressed in eqn (13) enables a direct assessment to be made of the need to consider creep crack growth effects. When the r.h.s. of eqn (13) is close to or greater than unity, failure is governed by the reference stress. The influence of a crack on failure time is then simply determined by its influence on the reference stress, i.e. from eqn (10)

by its influence on the limit load. Although eqn (13) is clearly incorrect when it predicts $t_i > t_r(\sigma_{ref})$ since $t_r(\sigma_{ref})$ is an upper bound on the final failure time[1], this is of little practical significance; tertiary creep strains could be included by using eqn (14) but if tertiary strains are important at the reference stress at t_i, then t_i must be close to $t_r(\sigma_{ref})$ and crack propagation can be neglected in determining final failure time.

It can be observed from eqn (13) that initiation is influenced both by material and size effects. Size effects are governed by the macroscopic distance R defined by eqn (11): for geometrically similar specimens R is directly proportional to specimen size; for small cracks in large components R is approximately proportional to crack size. Early initiation may be expected in materials with high secondary creep rates (high $\bar{\epsilon}$) and/or low values of initiation displacement δ_i. It should be recognized, however, that these material properties are unlikely to be independent as ductile materials with a high $\bar{\epsilon}$ may also exhibit a high δ_i and vice-versa for creep brittle materials. The stress exponent n is not particularly important in determining initiation and eqn (13) could be expressed as

$$t_i/t_r(\sigma_{ref}) = \frac{\alpha(n)}{\bar{\epsilon}}\left(\frac{\delta_i}{R}\right)^{n/n+1}. \tag{19}$$

From eqn (13) the value of α varies between 0.8 and 1.2 but as with the constant β in eqn (15) there may be a wider range shown by experimental results. Equation (19) should, however, give the correct functional dependence and for large n the important grouping becomes simply $(\delta_i/\bar{\epsilon}R)$.

Plastic and primary creep strains may be included approximately by using eqn (14) instead of eqn (13). This may be necessary for analysing results of laboratory tests at high stresses but should not be important at practical stress levels where safety factors against plastic collapse and creep rupture should ensure a value of σ_{ref} significantly lower than the yield stress. Initial strains are then only important when initiation occurs at low values of δ_i/R, i.e. at low total strain. As noted in Section 2.3 above, eqn (14) is not valid in these cases but since the predicted value of $t_i/t_r(\sigma_{ref})$ will then be small, for practical purposes initiation may be assumed to occur at $t = 0$ and an assessment based on crack growth.

4. COMPARISON WITH EXPERIMENTAL RESULTS

In this section the initiation times predicted by eqn (13) are compared with experimentally measured initiation times reported by Taylor and Batte[17] and Haigh[18]. Taylor and Batte[17] tested various sized double-edge notched specimens of a 1% Cr MoV steel. Tests were terminated prior to failure and the specimens examined metallographically to determine whether or not initiation had occurred. By testing a large number of specimens for different times and at different stresses an approximate boundary was determined between specimens which had initiated and those which had not. This boundary is shown in Fig. 2 which also includes plain specimen rupture data. It can be seen that initiation occurred at times considerably less than the rupture time at the reference stress. Taylor and Batte[17] measured the initiation displacement and found this to be sensibly constant at 2 μm for initiation times greater than 500 hr. An increase in initiation COD was found at shorter initiation times, i.e. in tests at higher stresses. The predictions of eqn (13) are shown in Fig. 2 for $\delta_i = 2\ \mu$m, $n = 7$, $\bar{\epsilon} = 2\%$ and $R = 5$ mm which is a typical value; the effect of allowing for the increased δ_i at short times is also shown. It can be seen that eqn (13) is in reasonable agreement with the initiation line estimated by Taylor and Batte[17]. A more detailed treatment of the individual data points is given in Fig. 3 where the different specimen geometries have been used in calculating R (see Appendix for details). The boundary between specimens which had initiated and those which had not is well described by eqn (13), some scatter occurring about the line but no obvious systematic errors in describing the widely different specimen geometries (R varying by a factor of 16) and initiation times (from 50 hr to in excess of 16000 hr). The scatter about the boundary $t/t_i = 1$ in Fig. 3 is comparable with the scatter about the boundary estimated in[17] and shown in Fig. 2. One point in Fig. 3 shows initiation at a time which is 0.38 times that predicted by eqn (13) but this specimen had edge cracks of significantly different sizes; allowing for the eccentricity of loading would increase the reference stress by about 10%, i.e. reduce the

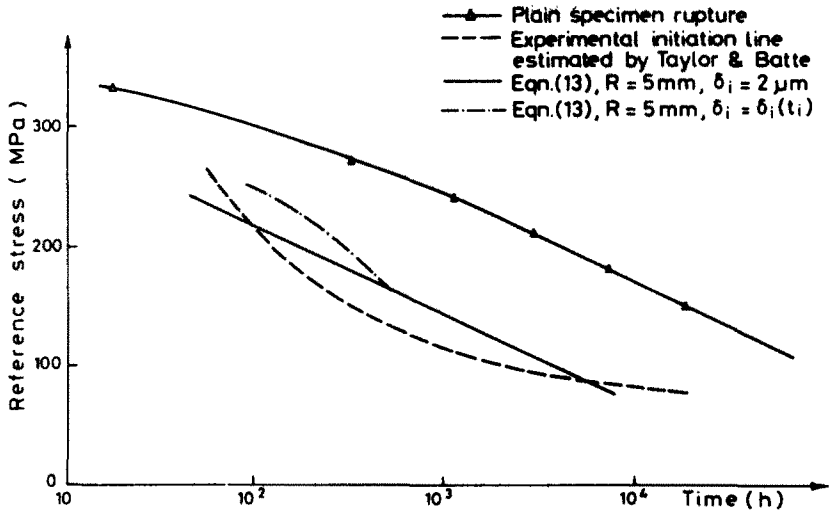

Fig. 2. Comparison of theory with experimental data of Taylor and Batte.

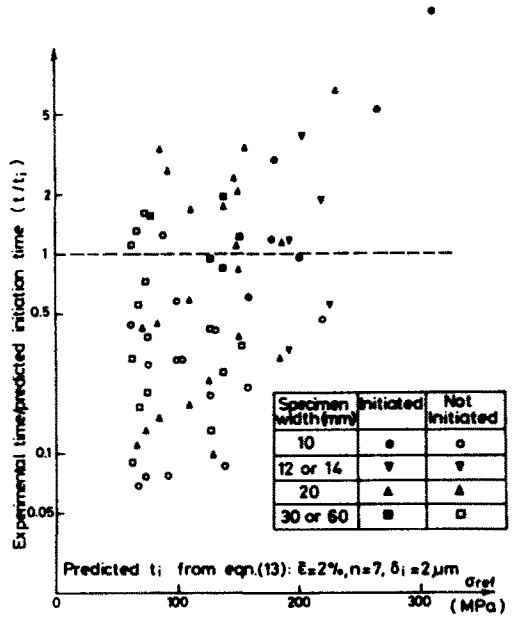

Fig. 3. Comparison of theory with experimental results of Taylor and Batte.

predicted initiation time by a factor of 2 so bringing the point within an acceptable scatter band.

Haigh[8] tested compact tension specimens of several Cr MoV steels. The experimental results for two different steels (Material 1 and Material 2 in Haigh's terminology) are given in Table 1 along with the predictions of eqn (13). Details of the analysis are given in the Appendix. Tests were performed on spark-machined slots so eqn (9) has been used to obtain the effective initiation COD $\bar{\delta}_i$ for use in eqn (13). It can be seen that the effective initiation COD is sensibly constant for each material, the value for material 1 being about twice that for material 2. The agreement between experimental and predicted values of $t_i/t_r(\sigma_{ref})$ is good for material 2 but not as good for material 1. The available creep strain data is at low stresses (154 MPa and less) and shows that for the same stress material 1 has a considerably lower creep strain rate than material 2. Thus since, in addition, the initiation COD in material 1 is twice that in material 2 a considerably longer initiation time would be expected in material 1 for the same load. It can be seen from Table 1 that this is not the case. This could simply be due to experimental scatter or it may suggest that at higher stresses ($\sigma_{ref} \sim 200$ MPa) the differences in the creep strain rates of the two materials are not as great as at lower stresses. There is insufficient materials data to

Table 1. Comparison of theory with experimental results of Haigh[8]

Material	Experimental Measurements					Predictions using eqn. (15)			
	σ_{ref} (MPa)	$t_r(\sigma_{ref})$ (h)	t_i (h)	$\frac{t_i}{t_r(\sigma_{ref})}$	$\delta_i-\delta_o$ (μm)	$\bar{\delta}_i$ (μm)	R (mm)	$\frac{t_i}{t_r(\sigma_{ref})}$	
1	172	2400	750	0.32	230	171	12	0.75	$\bar{\epsilon}$=2.5%
1	203	700	180	0.26	270	204	11	0.96	n=7
2	148	1900	550	0.29	105	71	11	0.32	$\bar{\epsilon}$=3%
2	169	820	250	0.31	125	86	11	0.38	n=7
2	203	250	130	0.52	120	82	11	0.36	

resolve this latter point. However, some experimental scatter may be expected as for $n = 7$ a factor of two difference in rupture time is caused by a change in reference stress of 10% which would be caused, for example, by a change in measured crack length of only 1.3 mm. Finally it may be noted that Goodall and Chubb[4] examined the final failure times of these specimens and found that they were reasonably well predicted by the creep rupture time at the reference stress; this conclusion would be drawn from the predicted initiation times for material 1.

CONCLUDING REMARKS

An expression has been derived which enables the time for initiation of creep crack growth to be determined from the COD at initiation and plain specimen creep strain and creep rupture data. The result has been normalised by the creep rupture time at the reference stress which is the lifetime which can be achieved when failure is governed by overall creep rupture mechanisms rather than by the initiation and growth of the crack. This enables a direct assessment of the importance on failure of crack tip dominated effects. Early initiation times may be expected in materials with low values of initiation COD and/or high values of the product of secondary creep rate and time to rupture. A size effect is also predicted with initiation occurring earlier in larger specimens for the same applied stress. There is encouraging agreement between the theoretical predictions and experimentally measured initiation times.

Acknowledgement—This paper is published by permission of the Central Electricity Generating Board.

REFERENCES

1. I. W. Goodall and R. D. H. Cockroft, On bounding the life of structures subjected to steady load and operating within the creep range. *Int. J. Mech. Sci.* **15**, 251 (1973).
2. I. W. Goodall, R. D. H. Cockroft and E. J. Chubb, An approximate description of the creep rupture of structures. *Int. J. Mech. Sci.* **17**, 351 (1975).
3. L. M. Kachanov, Rupture time under creep conditions. *Problems of Continuum Mechanics* (Edited by J. R. M. Radok). Society for Industrial and Applied Mathematics, Philadelphia (1961).
4. I. W. Goodall and E. J. Chubb, The creep ductile response of cracked structures. *Int. J. Fracture* **12**, 289 (1976).
5. J. R. Haigh, The mechanisms of macroscopic high temperature crack growth. Part II: Review and reanalysis of previous work. *Mater. Sci. Engng* **20**, 225 (1975).
6. E. G. Ellison and M. P. Harper, Creep behaviour of components containing cracks—a critical review. J. Strain Anal. **13**, 35 (1978).
7. R. A. Ainsworth, Some observations on creep crack growth, CEGB Report RD/B/N4868 (1980). *Int. J. Fracture* **18** (1982).
8. J. R. Haigh, The mechanisms of macroscopic high temperature crack growth, Part I: Experiments on tempered Cr MoV steels. *Mater. Sci. Engng* **20**, 213 (1975).
9. J. R. Rice, Mathematical analysis in the mechanics of fracture. *Fracture*, Vol. II (Edited by H. Liebowitz). Academic Press, New York (1968).
10. C. F. Shih, An engineering approach for examining crack growth and stability in flawed structures. CSNI Specialists Meeting on Tearing Instability, NUREG/CP-0010, CSNI Rep. 39 (1980).
11. R. K. Penny and D. L. Marriott, *Design for Creep*. McGraw-Hill, New York (1971).
12. D. J. F. Ewing, Strip yield models of creep crack incubation and growth. *Int. J. Fracture* **14**, 101 (1978).
13. R. M. McMeeking, Finite deformation analysis of crack-tip opening in elastic-plastic materials and implications for fracture. *J. Mech. Phys. Solids* **25**, 357 (1977).
14. J. L. Bassani and F. A. McClintock, Creep relaxation of stress around a crack tip. *Int. J. Solids Structures* **17**, 479 (1981).

15. I. W. Goodall, F. A. Leckie, A. R. S. Ponter and C. H. A. Townley, The development of high temperature design methods based on reference stresses and bounding theorems. *J. Engng Mat. Techn.* **101**, 349 (1979).
16. A. R. Dowling and C. H. A. Townley, The effects of defects on structural failure: a two-criteria approach. *Int. J. Pres. Ves. Piping* **3**, 77 (1975).
17. E. Taylor and A. D. Batte, Creep crack formation in a 1% Cr MoV rotor forging steel. *Int. Conf. on Engineering Aspects of Creep, I. Mech. E.*, Sheffield (1980).

APPENDIX ANALYSIS OF EXPERIMENTAL DATA

Data of Taylor and Batte[17]

The geometry tested by Taylor and Batte[17] was a double-edge cracked plate with crack lengths a and width 2b. The length parameter R of eqn (11) has been approximated as $R = K^2/\sigma^2_{ref}$. This approximation is quite accurate for a centre-cracked plate for moderate a/b and $n < 10$[7]. The reference stress has been taken as the net section stress with no allowance for eccentricity of loading when the edge cracks are of different lengths. The stress intensity factor has been calculated according to the formula.

$$K = \sigma\sqrt{(\pi a)}\{1.12 + 0.2(a/b) - 1.2(a/b)^2 + 1.93(a/b)^3\}$$

where σ is the gross section stress and a has been taken as the length of the longer of the two edge-cracks. Detailed analysis of the data leads to values of R ranging from 1.1 to 18.8 mm. A typical value $R = 5$ mm has been used for the prediction in Fig. 2.

The plain specimen data may be reasonably represented by $n = 7$ and $\bar{\epsilon} = 2\%$. It can be seen from Fig. 2 that considerable extrapolation of the rupture data is required for stresses less than about 100 MPa so that the predicted initiation times used in Fig. 3 are only approximate at low stresses. The COD at initiation is sensibly constant at 2 μm for initiation times greater than 500 hr (see Fig. 6 of [17]). The solid curve of Fig. 2 and Fig. 3 have been produced using this value of $\delta_i = 2$ μm. The effect of allowing for the increase in δ_i at short t_i (see [17], Fig. 6; e.g. $\delta_i = 7$ μm at $t_i = 100$ hr) is shown in Fig. 2. Using a larger δ_i at small t_i reduces some values of (t/t_i) in Fig. 3 but makes no significant difference to the boundary between specimens which had initiated and those which had not. It may be noted that the effect at short t_i may not be as great as that depicted in Fig. 2 as the increase in δ_i at high stresses may also be associated with increases in $\bar{\epsilon}$ and n, although on the basis of high stress data Ewing[12] used $\bar{\epsilon} = 2.22\%$ and $n = 10$ which are close to the values used here.

Data of Haigh[8]

Haigh tested compact tension specimens of width 65 mm and net thickness 22.5 mm. Values of reference stress for these tests have been calculated by Goodall and Chubb[4] and these are reproduced in Table 1. Values of C^* for this geometry have been tabulated by Shih[10] for various stress indeces n. The value $n = 7$ has been used in the present calculations for both materials 1 and 2 and the resulting values of the geometrical parameter R of eqn (11) are given in Table 1. It may be noted that Shih[10] expresses his results in a form which is essentially

$$C^* = \sigma'_{ref}\dot{\epsilon}(\sigma'_{ref})(w - a)h_1(a/w, n)$$

where a is crack length, w is specimen width, h_1 is a function which is tabulated, and σ'_{ref} is defined according to eqn (10) but using a different expression for limit load to that used by Goodall and Chubb[4]. Equation (11) then gives

$$R = (w - a)h_1(a/w, n)(\sigma'_{ref}/\sigma_{ref})^{n+1}.$$

The reference stress obtained in[4] is based on experimental evidence and is preferred here. The comparison between experimental and predicted values of $t_i/t_r(\sigma_{ref})$ is, however, not affected by the choice of limit load expression used to define σ_{ref}: a change in σ_{ref} changes R and hence the predicted t_i/t_r of eqn (13) but the change in σ_{ref} also changes $t_r(\sigma_{ref})$ and hence the experimental t_i/t_r. If σ'_{ref} had been used in calculating the results in Table 1 the experimental and predicted values of $t_i/t_r(\sigma_{ref})$ would both have been reduced by about 40%.

For material 1 the plain specimen strain and rupture data has been represented by $n = 7$ and $\bar{\epsilon} = 2.5\%$. The value $n = 7$ is a good fit to the rupture data and $\bar{\epsilon} = 2.5\%$ has been suggested by Ewing[12] (see Table 4 of that paper). For material 2 the value $n = 7$ is again a good fit to the rupture data and $\bar{\epsilon} = 3\%$ appears a reasonable fit to the limited strain data in[8]. In calculating the effective COD, $\bar{\delta}_i$, using eqn (9) the initial spark-machined notch has been assumed to be of radius $\delta_0/2 = 260$ μm (see [8]).